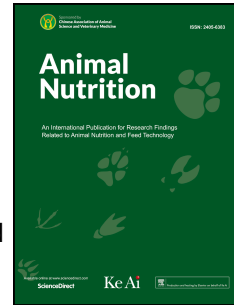


Journal Pre-proof

Localization of urea transporter B in the developing bovine rumen

Chongliang Zhong, Tamsin Lyons, Orla Heussaff, Evelyn Doyle, Eoin O'Hara, Sinead M. Waters, David Kenny, Gavin S. Stewart



PII: S2405-6545(22)00051-8

DOI: <https://doi.org/10.1016/j.aninu.2022.03.006>

Reference: ANINU 599

To appear in: *Animal Nutrition Journal*

Received Date: 1 May 2021

Revised Date: 2 March 2022

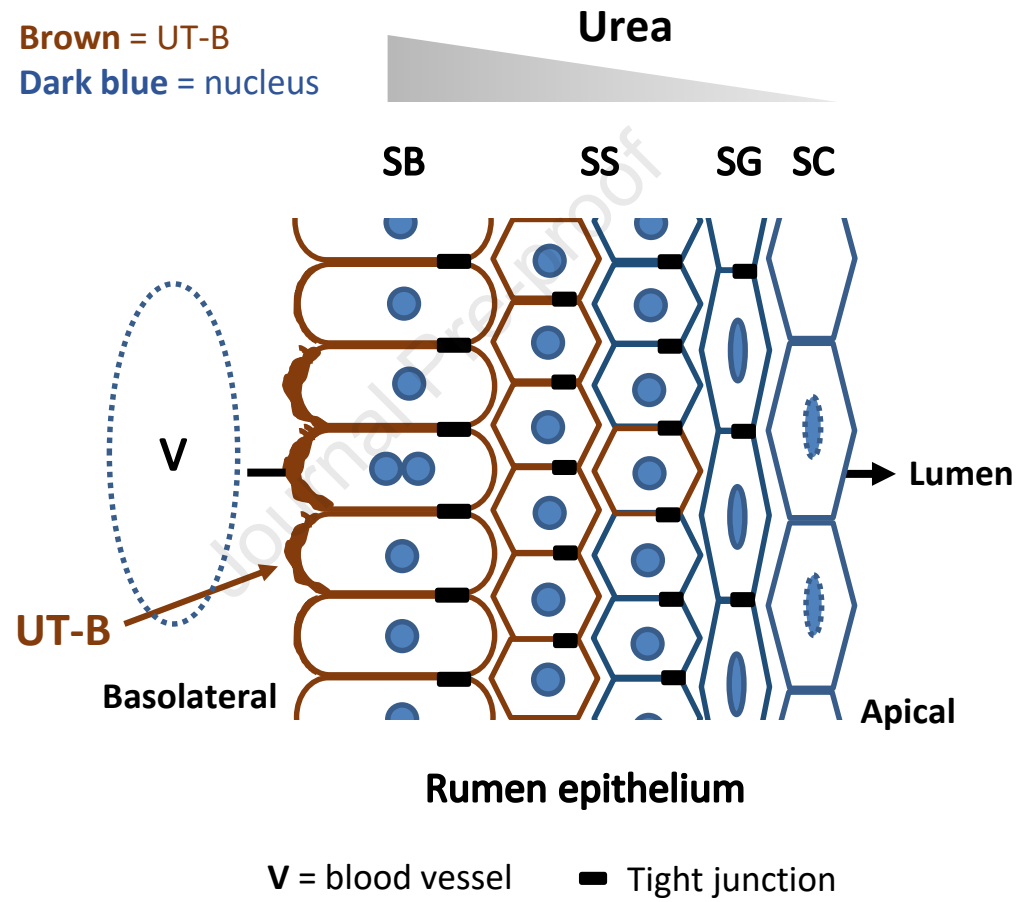
Accepted Date: 29 March 2022

Please cite this article as: Zhong C, Lyons T, Heussaff O, Doyle E, O'Hara E, Waters SM, Kenny D, Stewart GS, Localization of urea transporter B in the developing bovine rumen, *Animal Nutrition Journal*, <https://doi.org/10.1016/j.aninu.2022.03.006>.

This is a PDF file of an article that has undergone enhancements after acceptance, such as the addition of a cover page and metadata, and formatting for readability, but it is not yet the definitive version of record. This version will undergo additional copyediting, typesetting and review before it is published in its final form, but we are providing this version to give early visibility of the article. Please note that, during the production process, errors may be discovered which could affect the content, and all legal disclaimers that apply to the journal pertain.

© 2022 Chinese Association of Animal Science and Veterinary Medicine. Publishing services by Elsevier B.V. on behalf of KeAi Communications Co. Ltd.

Rumen UT-B urea transporter development



1 **Localization of urea transporter B in the developing bovine rumen**

2

3 Chongliang Zhong ^a, Tamsin Lyons ^a, Orla Heussaff ^a, Evelyn Doyle ^a, Eoin O’Hara ^{b, c}, Sinead
4 M. Waters ^b, David Kenny ^b, Gavin S. Stewart ^{a, *}

5

6 ^aSchool of Biology and Environmental Science, University College Dublin, Belfield, Dublin 4,
7 Ireland

8 ^bAnimal and Bioscience Research Department, Animal and Grassland Research and Innovation
9 Centre, Teagasc, Grange, County Meath, Ireland

10 ^cDepartment of Agriculture, Food, and Nutritional Sciences, University of Alberta, Edmonton,
11 Alberta, Canada

12

13 *Corresponding author.

14 Email address: gavin.stewart@ucd.ie (G. S. Stewart)

15

16

17 Abstract

18 Urea nitrogen secreted from blood to rumen is a crucial factor shaping the symbiotic
19 relationship between host ruminants and their microbial populations. Passage of urea across
20 rumen epithelia is facilitated by urea transporter B (UT-B), but the long-term regulation of these
21 proteins remains unclear. As ruminal function develops over a period of months, the developing
22 rumen is an excellent model with which to investigate this regulation. Using rumen epithelium
23 samples of calves from birth to 96 d of age, this study performed immunolocalization studies to
24 localize and semi-quantify UT-B protein development. As expected, preliminary experiments
25 confirmed that ruminal monocarboxylate transporter 1 (MCT1) short chain fatty acid transporter
26 protein abundance increased with age ($P < 0.01$, $n = 4$). Further investigation revealed that
27 ruminal UT-B was present in the first few weeks of life and initially detected in the basolateral
28 membrane of stratum basale cells. Over the next 2 months, UT-B staining spread to other
29 epithelial layers and semi-quantification indicated that UT-B abundance significantly increased
30 with age ($P < 0.01$, $n = 4$ or 6). These changes were in line with the development of rumen
31 function after the advent of solid feed intake and weaning, exhibiting a similar pattern to both
32 MCT1 transporters and papillae growth. This study therefore confirmed age-dependent changes
33 of in situ ruminal UT-B protein, adding to our understanding of the long-term regulation of
34 ruminal urea transporters.

35

36 **Keywords:** UT-B, Immunolocalization, Rumen, Bovine, Development

37

38

39 **1. Introduction**

40 The rumen ecosystem represents a classic example of a symbiotic relationship between
41 host animals and microbial populations (Morais & Mizrahi, 2019). Since animals and commensal
42 gut microbes are constantly exposed to limited nitrogen resources, nitrogen in the gastrointestinal
43 tract is a crucial factor shaping this relationship (Reese et al., 2018) and is a fundamental driver
44 of host-microbiome interactions (Holmes et al., 2017). Mechanisms have evolved in this low
45 nitrogen setting to conserve nitrogen and maintain the symbiotic relationship with microbes. One
46 important example is the urea nitrogen salvaging (UNS) process, through which ruminants can
47 shift urea excretion from kidney to rumen (40% to 80% of synthesised urea) and where ureolytic
48 bacteria adhering to the rumen wall can break urea down into ammonia (Stewart and Smith,
49 2005). This ammonia is used as a nitrogen resource for synthesis of microbial proteins, which
50 provide a substantial metabolizable protein supply to the ruminant host (Stewart and Smith,
51 2005).

52 It has long been established that the entry of urea into the rumen is facilitated by urea
53 transporter B2 (UT-B2) (Stewart et al., 2005; Coyle et al., 2016; Zhong et al., 2020). Unlike
54 renal UT-A-mediated urea transport, UT-B2-mediated trans-cellular urea transport is
55 constitutively activated and unaffected by known UT-A regulators, such as vasopressin (Tickle
56 et al., 2009). Nevertheless, it remains unclear how the urea transport capacity of rumen epithelia
57 is regulated through the UT-B2 proteins. Previous studies of the regulation of ruminal urea
58 transporters have mainly focused on manipulating diets of adult animals by altering dietary
59 nitrogen levels. However, only weak associations have been found between urea flux across
60 rumen and urea transporters under different dietary nitrogen levels (Marini and Van Amburgh,
61 2003; Marini et al., 2004; Ludden et al., 2009; Kristensen et al., 2010). Increasingly, studies have

62 shown that UT-B transporters are more responsive to the changes of dietary energy levels and
63 correlated with the resulting microbial short chain fatty acids (SCFA) (Simmons et al., 2009;
64 Walpole et al., 2015). These results are in line with various ex vivo functional studies showing
65 that urea transport capacity of rumen epithelium can be regulated by pH in the presence of SCFA
66 and CO₂ (Abdoun et al., 2010; Lu et al., 2014). It has also been shown that SCFA and pH can
67 regulate UT-B abundance in rumen-derived primary cells (Lu et al., 2015). These findings
68 support the idea that urea plays a key physiological role in buffering microbially-derived SCFA
69 in the rumen. In this process, ammonia produced from urea by bacterial urease can combine with
70 H⁺ ions to form ammonium ions, which can then be readily reabsorbed across the rumen
71 epithelia (Stumpff, 2018).

72 Calves undergo a transition from pre-ruminant to ruminant, during which microbial
73 colonization, fermentation capacity and need for UNS all increase (Stewart and Smith, 2005).
74 The developing rumen is therefore an excellent in vivo model to observe the regulation of urea
75 transporters. Indeed, Berends et al. quantified that the salvaged urea nitrogen contributes to 19%
76 of nitrogen retention during the transition from pre-ruminants (milk fed calves) to ruminants
77 (solid feed fed calves) (Berends et al., 2014). Importantly, in line with this, the *UT-B* mRNA
78 expression also increased with solid feed intake (Berends et al., 2014). This again suggests
79 microbial fermentation activity and derived production of SCFA might be the key long-term
80 regulator of ruminal urea transporters. However, the protein localization and abundance of UT-B
81 were not investigated. This current study therefore aimed to localize and semi-quantify in situ
82 protein abundance of UT-B in the developing bovine rumen.

83 2. Materials and methods

84 2.1 Animals and tissue samples

85 All procedures were approved by the Teagasc Animal Ethics Committee and conducted
86 under experimental license from the Irish Health Products Regulatory Authority, in accordance
87 with the Cruelty to Animals Act 1876 and the European Communities (Amendments of the
88 Cruelty to Animals Act 1876) Regulations, 1994. The full details of this animal model using
89 Aberdeen Angus heifers have been previously published (O'Hara et al., 2020). Briefly, before
90 birth and irrespective of sex, calves were assigned to one of 6 groups and based on this they were
91 euthanized at birth (D0, $n = 4$), at d 7 (D7, $n = 4$), 14 (D14, $n = 4$), 21 (D21, $n = 4$), 28 (D28, n
92 = 4), or 96 (D96, $n = 6$) after birth. Calves not euthanized at birth could suckle their dam for 2 d
93 post birth, at which point they were removed and penned individually. Calves were then reared
94 on milk replacer (5 L/d, fed twice daily). From D7 onwards, calves had access to ad libitum
95 concentrate. Calves were weaned at the age of 56 d (or earlier if consuming 1 kg concentrates per
96 day for 3 consecutive days). After weaning, calves were offered 2 kg concentrate per day, with
97 ad libitum water and hay, until they were euthanized at D96. Following euthanasia, samples of
98 ventral sac rumen tissue were taken, washed in phosphate buffer solution, and fixed in 10%
99 neutral buffered formalin. After fixation, samples were dehydrated with increasing
100 concentrations of ethyl-alcohol (50% to 100%) using an automated processor (Tissue-TEK VIP,
101 Sakura, Finetek) and embedded in paraffin wax.

102

103 2.2 Hematoxylin-eosin (HE)-staining and papillae measurements

104 The paraffin-embedded calf rumen tissues were cut into 4- μ m sections using a microtome
105 (Leitz RM2255) and mounted onto negatively charged glass slides. Samples were then stained
106 with haematoxylin and eosin (HE) using a Leica auto-stainer (Leica ST5020) and observed using
107 a light microscope (Leica DM3000). Measurements of papillae length and width were taken at
108 50 \times magnification using a 1-cm graticule, with 10 well-orientated papillae measured per section.
109 Tissue sections harvested from calves at birth (D0) had fewer papillae present, with only 4
110 available per section for measurement compared to the minimum of 10 measured per section
111 from all other time points. Papilla length was measured from the tip to the base of the papilla
112 (adjacent to the tunica muscularis layer). Papilla width was measured at the midpoint of the
113 papilla, from the outside epithelial edges.

114

115 *2.3 Immunohistochemistry and protein abundance score*

116 Rumen papillae sections of 5 μ m were cut and attached to slides (Thermo Scientific,
117 Hungary). After overnight drying, sections were de-waxed in Neo-clear (Millipore, Germany),
118 and rehydrated in a series of decreasing ethanol concentrations (100%, 90% and 70%). Sections
119 were incubated in 0.3% (Vol/Vol) H₂O₂ in methanol at room temperature for 30 min. and
120 washed (3 \times 10 min) in d 1 washing buffer containing 1% (Wt/Vol) bovine serum albumin
121 (BSA), 0.2% (Vol/Vol) gelatine, 0.05% (Wt/Vol) saponin in phosphate buffered solution (PBS).
122 They were incubated overnight at 4 °C in UT-B (1:250; hUTBc19) (Walpole et al., 2014) or
123 monocarboxylate transporter 1 (MCT1) antibodies (1:2,000; AB1286-I, Millipore) diluted in a
124 buffer containing 0.1% (Wt/Vol) BSA, 0.3% (Vol/Vol) Triton X-100 in PBS. Sections were then
125 washed (3 \times 10 min) in d 2 washing buffer containing 0.1% (Wt/Vol) BSA, 0.2% (Vol/Vol)
126 gelatine, 0.05% (Wt/Vol) saponin in PBS, followed by incubation with a horseradish peroxidase-

127 linked anti-rabbit secondary antibody at a dilution of 1:200 (for UT-B) or an anti-chicken
128 antibody at 1:2,000 (for MCT1) for 1 h at room temperature. After further washes, sections were
129 reacted with 3,3'-diaminobenzidine (Sigma-Aldrich, USA) for 10 min and counterstained with
130 haematoxylin. After serial dehydration in ethanol (70%, 90% and 100%), stained sections were
131 preserved using a mounting medium (Eukitt, Sigma-Aldrich, Germany) and coverslips. Negative
132 controls were performed by replacing the primary antibody with its dilution buffer. For peptide
133 competition analysis, UT-B primary antibody was pre-absorbed with its immunizing peptide (1
134 $\mu\text{g}/\mu\text{L}$) for 24 h or an equivalent amount of an irrelevant peptide.

135 Stained slides were examined under a light microscope (Leica, Germany) and
136 representative staining was imaged, using a digital camera (DFC420C, Leica, Germany) with its
137 software (Application Suit V4). To semi-quantitatively determine in situ protein abundance,
138 signal strength was “blind” scored by 3 experienced examiners on a scale of 0 to 5, where 0 =
139 none, 1 = very weak, 2 = weak, 3 = moderate, 4 = strong, and 5 = very strong. For each animal,
140 the scores of the 3 examiners were averaged.

141

142 *2.4 Statistical analysis*

143 Data were visualized using “ggplot2” package in R software environment. General linear
144 models were used to test null hypotheses:

$$145 \quad \text{Papillae length} = \beta_{\text{age}} + N(0, \sigma_i),$$

$$146 \quad \log(\text{Papillae width}) = \beta_{\text{age}} + N(0, \sigma_i);$$

$$147 \quad \text{UT-B expression score} = \beta_{\text{age}} + N(0, \sigma_i),$$

148 Where β_{age} was the fitted effects of ages on the response, and $N(0, \sigma_i)$ was the normally
149 distributed error with zero mean and standard deviation σ_i . The models were fitted to the data by
150 maximum likelihood using R statistical software (R Core Team 2018). Residuals of these fitted
151 models were consistent with model assumptions of normality, homogeneity of variance and
152 independence. Once differences were found, *post hoc* testing was performed using Tukey's HSD
153 to test for differences between each pair of ages. When data transformation was made to meet
154 model assumptions, original data were used to make box and dot plot, whereas *P*-value and
155 estimated means were derived from transformed data (estimated means were back transformed).
156 Hypothesis tests used a critical significance level of 5%.

157 3. Results

158 To examine the morphological development of calf rumen epithelia, sections were
159 stained using a HE method (Fig. 1A). Papillae length and width were both measured and found
160 to differ with age (ANOVA, $P < 0.01$, $n = 3$; Fig. 1B). Papillae in the rumen of D96 calves
161 (approximately 1,350 μm) were 4-fold longer than that of D0 calves (approximately 330 μm , $P <$
162 0.01 , Tukey's HSD; Fig. 1B). In contrast, no differences of length were found among the ages of
163 0, 7, 14, 21, and 28 d ($P > 0.05$; Fig. 1B). Papillae width was greater in D21 (approximately 190
164 μm , $P < 0.01$, Tukey's test), D28 (approximately 160 μm , $P < 0.05$), and D96 (approximately 290
165 μm , $P < 0.01$) calves compared to D0 calves (approximately 70 μm ; Fig. 1B).

166 For immunolocalization protocol validation, we first investigated the ruminal SCFA
167 transporter MCT1 - previously shown to increase with age at both mRNA and protein levels
168 (Flaga et al., 2015). In the D0 animals, weak staining was dispersed in the cytoplasm throughout
169 all epithelial cell layers (Fig. 2A). For D7 to D28 tissues, MCT1 signals were accumulated at the
170 cell membrane of stratum basale cells, particularly the basolateral membrane (Fig. 2B, D28). For

171 D96, strong cell membrane staining was detected throughout basale and spinosum layers (Fig.
172 2C). Statistical analysis confirmed a highly significant increase in “blind-scored” MCT1 staining
173 as the rumen developed ($P < 0.01$, $n = 4$) (Fig. 2D).

174 Next, the cellular localization of UT-B protein was investigated and in D0 tissues only
175 faint, cytoplasmic staining was observed (4 out of 4 animals) (Fig. 3A). For D7 to D28, positive
176 immunostaining was frequently observed in the stratum basale (11 out of 16 animals),
177 particularly at the basolateral side (Fig. 3B, D21). At D96, stronger signals were found in the cell
178 membranes of the stratum basale (5 out of 6 animals) and sometimes the stratum spinosum (3 out
179 of 6 animals) (Fig. 3C). Statistical analysis again showed highly significant differences across
180 ages ($P < 0.01$, $n = 4$ or 6), with the highest scores at D96 and lowest at D0 ($P < 0.01$, Tukey’s
181 HSD; Fig. 3D). In addition, Pearson correlation coefficient analysis showed strong correlations
182 between UT-B scores and (i) papillae length (0.91), (ii) papillae width (0.82), and most
183 interestingly, (iii) MCT1 scores (0.83).

184 Finally, to confirm UT-B staining specificity, antibody removal and peptide competition
185 analysis was performed. Sequential incubation with UT-B and secondary antibodies produced
186 strong staining across epithelial layers (Fig. 4A), whereas no signals occurred in the absence of
187 the UT-B antibody (Fig. 4B). Pre-incubation with the UT-B immunizing peptide prevented any
188 staining (Fig. 4C), whereas using an equivalent amount of an unrelated peptide had minimal
189 effect (Fig. 4D). Interestingly, UT-B staining was often seen to be strongest in basolateral
190 membranes of the stratum basale cells nearest to blood vessels (Fig. 4D; Fig. 4E).

191

192 4. Discussion

193 Our previous studies have suggested that investigations of ruminal urea transporters
194 should always consider potential alterations at the tissue level (Simmons et al., 2009; Coyle et
195 al., 2016), as well as the cellular level, considering the rumen's highly adaptable morphological
196 response to dietary change. In this current study, we measured the papillae length and width to
197 confirm the basic morphology development of rumen epithelium across ages. In the first month
198 after birth, the rumen epithelium had only slightly developed, potentially initiated by the ad
199 libitum solid feed intake and the resulting fermentation product of SCFA (Flatt et al., 1958;
200 Sander et al., 1959; Tamate et al., 1962). The papillae were short in length and width, with
201 multiple epithelial cells that were small and concisely packed (D14). In contrast, by the third
202 month (D96) the papillae had significantly developed with 4-fold increases in both length and
203 width, due to weaning which occurred at d 56. It should be noted that whilst our simplified
204 procedure to measure papillae was not optimal (cf. measuring dissected papillae), it was
205 sufficient for simply confirming the well-established papillae growth that occurs during rumen
206 development. Although the papillae were still smaller than the measurements commonly reported
207 in adult cows (Coyle et al., 2016), the structure was similar. The epithelial cells had formed the
208 defined shapes of the 4 layers – stratum basale, stratum spinosum, stratum granulosum and
209 stratum corneum (D96) – seen in well-developed rumen epithelia. Denser barrier, balloon cells,
210 and the extensive vascular system (mainly venules with fenestrated endothelium) were also
211 observed.

212 We next investigated the localization of MCT1 transporters, which transport SCFA
213 across rumen papillae layers and have an expression pattern associated with ruminal microbial
214 fermentation capacity (Flaga et al., 2015). Our data confirmed MCT1 protein predominantly

215 located in the cell membranes of stratum basale and stratum spinosum. The developmental
216 pattern observed was the same as a previous study that comprehensively investigated MCT1
217 mRNA expression, protein abundance and localization (Flaga et al., 2015) - namely that MCT1
218 protein increases with age, in association with increased microbially-derived SCFA levels. We
219 suggest that these data validate our use of the blind-scored immunolocalization protocol to semi-
220 quantify the relative levels of ruminal transporter protein.

221 Our next set of immunolocalization data illustrated where UT-B protein began to develop
222 within the rumen papillae. UT-B protein was frequently observed at the stratum basale cells of
223 the undeveloped papillae and only extended to the stratum spinosum of the more developed
224 papillae. Furthermore, even observed in some of the developed D96 tissues, the most prominent
225 staining was at basolateral membranes of stratum basale cells facing blood vessels – a predicted
226 physiological necessity for moving urea from the blood into the rumen.

227 Although our UT-B immunolocalization data confirmed an age-dependent change of in
228 situ UT-B protein abundance, the pattern was not a simple linear increase. Instead, it
229 corresponded with the 3 phases of calves' life – namely birth (D0, pre-ruminant), pre-weaning
230 (D7 to D28; transition period) and post-weaning (D96, ruminant). This indicated the apparent
231 stimuli of enhanced UT-B protein abundance to be solid feed intake and weaning. Interestingly, a
232 previous study showed that providing solid feed intake produced a quadratic increase in UT-B
233 mRNA expression - with a dramatic 5-fold increase at the initial provision, then a slight change
234 with the increase of solid feed intake (Berends et al., 2014). This suggested that a change of
235 ruminal local conditions, especially abrupt changes, have dramatic effects on ruminal UT-B
236 mRNA expression. Our findings strongly suggest that similar changes occur with UT-B protein
237 abundance, although perhaps over a more prolonged duration. Finally, it is particularly

238 noteworthy that there was such a strong correlation (0.83) between the immunostaining scores
239 obtained for UT-B and MCT1. This suggests very similar regulatory factors are likely to be
240 involved in controlling the ruminal abundance of these 2 transporters (e.g. SCFA concentration).

241 It has recently been suggested that microbially-derived SCFA, especially butyrate, might
242 be the direct regulator of rumen urea transport via changing UT-B expression (Lu et al., 2019).
243 SCFA were not measured in this study, but we speculate that the free access to concentrate diet
244 from D7 to D28 enhanced microbial fermentation activity and could explain the initial increase
245 of UT-B protein abundance. As the calves still rely on milk replacer at these stages, rumen
246 function had not reached full capacity and UT-B protein abundance was moderate. From D56
247 onwards, calves were weaned and fed on concentrate and hay. By D96, the rumen function was
248 greater, now playing a major role in digestion and hence UT-B protein was required at higher
249 levels. From the findings of this initial study, we now believe extensive future studies are
250 required that i) involve larger numbers of calves, ii) undertake precise measurements of papillae
251 size, dietary intake and ruminal SCFA concentrations, iii) utilize additional techniques to analyze
252 transporter mRNA expression (i.e. real-time PCR) and protein abundance (i.e. Western blotting),
253 and iv) investigate the potential important effect of biological sex on the regulation of ruminal
254 UT-B transporters.

255 **5. Conclusions**

256 This study has characterized UT-B protein localization and abundance in the developing
257 rumen. The UT-B localization pattern agrees well with a functional role of transporting urea
258 from the blood to the rumen, with the age-dependent increases in protein abundance supporting
259 the idea that UT-B regulation occurs directly in response to levels of ruminal SCFA. These

260 findings therefore appear to confirm UT-B involvement in the functioning of the developing
261 bovine rumen.

262 **Author contributions**

263 **Chongliang Zhong**: conceptualization, formal analysis, investigation, funding, writing – original
264 draft preparation. **Tamsin Lyons**: investigation, writing – original draft. **Orla Heussaff**:
265 validation, investigation. **Evelyn Doyle**: methodology, writing – review and editing, funding.
266 **Eoin O’Hara**: methodology, writing – review and editing. **Sinead Waters**: methodology,
267 writing – review and editing, funding. **David Kenny**: methodology, writing – review and editing,
268 funding. **Gavin Stewart**: conceptualization, writing – original draft preparation, supervision,
269 funding.

270

271

272 Declaration of competing interest

273 The authors declare that there is no conflict of interest.

274 Acknowledgements

275 The authors would like to thank Dr. Carl Ng, Ms. Frances Downey, Dr. Carlotta Sacchi
276 and Dr. Alan Farrell for their technical assistance throughout this study. The authors are also
277 grateful to the scholarship funding (CZ) from The China Scholarship Council and University
278 College Dublin.

279

280

281 **References**

- 282 Abdoun K, Stumpff F, Rabbani I, Martens H. Modulation of urea transport across sheep rumen
283 epithelium in vitro by SCFA and CO₂. *Am J Physiol - Gastrointest Liver Physiol*
284 2010;298:G190–G202.
- 285 Berends H, van den Borne JJGC, Røjen BA, van Baal J, Gerrits WJJ. Urea recycling contributes
286 to nitrogen retention in calves fed milk replacer and low-Protein solid feed. *J Nutr*
287 2014;144:1043–1049.
- 288 Coyle J, McDaid S, Walpole C, Stewart GS. UT-B Urea transporter localization in the bovine
289 gastrointestinal tract. *J Membr Biol* 2016;249:77–85.
- 290 Flaga J, Górká P, Zabielski R, Kowalski ZM. Differences in monocarboxylic acid transporter
291 type 1 expression in rumen epithelium of newborn calves due to age and milk or milk
292 replacer feeding. *J Anim Physiol Anim Nutr (Berl)* 2015;99:521–530.
- 293 Flatt WP, Warner RG, Loosli JK. Influence of purified materials on the development of the
294 ruminant stomach. *J Dairy Sci* 1958;41:1593–1600.
- 295 Holmes AJ, Chew YV, Colakoglu F, Cliff JB, Klaassens E, Read MN, Solon-Biet SM,
296 McMahon AC, Cogger VC, Ruohonen K, Raubenheimer D, Le Couteur DG, Simpson SJ.
297 Diet-microbiome interactions in health are controlled by intestinal nitrogen source
298 constraints. *Cell Metab* 2017;25:140–151.
- 299 Kristensen NB, Storm AC, Larsen M. Effect of dietary nitrogen content and intravenous urea
300 infusion on ruminal and portal-drained visceral extraction of arterial urea in lactating
301 Holstein cows. *J Dairy Sci* 2010;93:2670–2683.
- 302 Lu Z, Stumpff F, Deiner C, Rosendahl J, Braun H, Abdoun K, Aschenbach JR, Martens H.
303 Modulation of sheep ruminal urea transport by ammonia and pH. *Am J Physiol Integr*

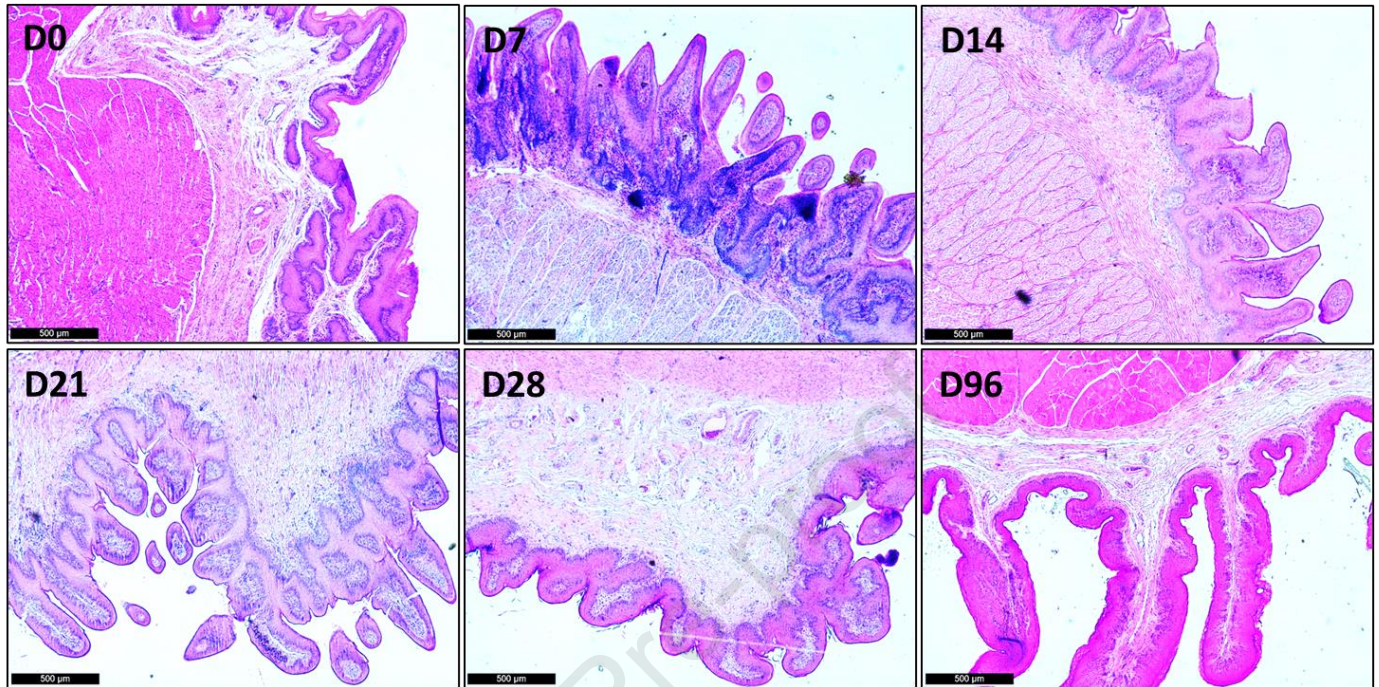
- 304 Comp Physiol 2014;307:R558–R570.
- 305 Lu Z, Gui H, Yao L, Yan L, Martens H, Aschenbach JR, Shen Z. Short-chain fatty acids and
306 acidic pH upregulate UT-B, GPR41, and GPR4 in rumen epithelial cells of goats. *Am J*
307 *Physiol - Regul Integr Comp Physiol* 2015;308:R283–R293.
- 308 Lu Z, Shen H, Shen Z. Effects of dietary-SCFA on microbial protein synthesis and urinal urea-N
309 excretion are related to microbiota diversity in rumen. *Front Physiol* 2019;10:1079.
- 310 Ludden PA, Stohrer RM, Austin KJ, Atkinson RL, Belden EL, Harlow HJ. Effect of protein
311 supplementation on expression and distribution of urea transporter-B in lambs fed low-
312 quality forage. *J Anim Sci* 2009;87:1354–1365.
- 313 Marini JC, Klein JD, Sands JM, Van Amburgh ME. Effect of nitrogen intake on nitrogen
314 recycling and urea transporter abundance in lambs. *J Anim Sci* 2004;82:1157–1164.
- 315 Marini JC, Van Amburgh ME. Nitrogen metabolism and recycling in Holstein heifers. *J Anim*
316 *Sci* 2003;81:545–552.
- 317 Moraïs S, Mizrahi I. The road not taken: The rumen microbiome, functional groups and
318 community states. *Trends Microbiol* 2019;27:538–549.
- 319 O’Hara E, Kenny DA, McGovern E, Byrne CJ, McCabe MS, Guan LL, Waters SM.
320 Investigating temporal microbial dynamics in the rumen of beef calves raised on two farms
321 during early life. *FEMS Microbiol Ecol* 2020;96:1–16.
- 322 Reese AT, Pereira FC, Schintlmeister A, Berry D, Wagner M, Hale LP, Wu A, Jiang S, Durand
323 HK, Zhou X, Premont RT, Diehl AM, O’Connell TM, Alberts SC, Kartzinel TR, Pringle
324 RM, Dunn RR, Wright JP, David LA. Microbial nitrogen limitation in the mammalian large
325 intestine. *Nat Microbiol* 2018;3:1441–1450.
- 326 Sander EG, Warner RG, Harrison HN, Loosli JK. The stimulatory effect of sodium butyrate and

- 327 sodium propionate on the development of rumen mucosa in the young calf. *J Dairy Sci*
328 1959;42:1600–1605.
- 329 Simmons NL, Chaudhry AS, Graham C, Scriven ES, Thistlethwaite A, Smith CP, Stewart GS.
330 Dietary regulation of ruminal bovine UT-B urea transporter expression and localization. *J*
331 *Anim Sci* 2009;87:3288–3299.
- 332 Stewart GS, Graham C, Cattell S, Smith TPL, Simmons NL, Smith CP. UT-B is expressed in
333 bovine rumen: potential role in ruminal urea transport. *Am J Physiol Integr Comp Physiol*
334 2005;289:R605–R612.
- 335 Stewart GS, Smith CP. Urea nitrogen salvage mechanisms and their relevance to ruminants, non-
336 ruminants and man. *Nutr Res Rev* 2005;18:49–62.
- 337 Stumpff F. A look at the smelly side of physiology: transport of short chain fatty acids. *Pflugers*
338 *Arch Eur J Physiol* 2018;470:571–598.
- 339 Tamate H, McGilliard AD, Jacobson NL, Getty R. Effect of various dietaries on the anatomical
340 development of the stomach in the calf. *J Dairy Sci* 1962;45:408–420.
- 341 Tickle P, Thistlethwaite A, Smith CP, Stewart GS. Novel bUT-B2 urea transporter isoform is
342 constitutively activated. *Am J Physiol Integr Comp Physiol* 2009;297:R323–R329.
- 343 Walpole C, Farrell A, McGrane A, Stewart GS. Expression and localization of a UT-B urea
344 transporter in the human bladder. *Am J Physiol - Ren Physiol* 2014;307:F1088–F1094.
- 345 Walpole ME, Schurmann BL, Górka P, Penner GB, Loewen ME, Mutsvangwa T. Serosal-to-
346 mucosal urea flux across the isolated ruminal epithelium is mediated via urea transporter-B
347 and aquaporins when Holstein calves are abruptly changed to a moderately fermentable
348 diet. *J Dairy Sci* 2015;98:1204–1213.
- 349 Zhong C, Farrell A, Stewart GS. Localization of aquaporin-3 proteins in the bovine rumen. *J*

350 Dairy Sci 2020;103:2814–2820.

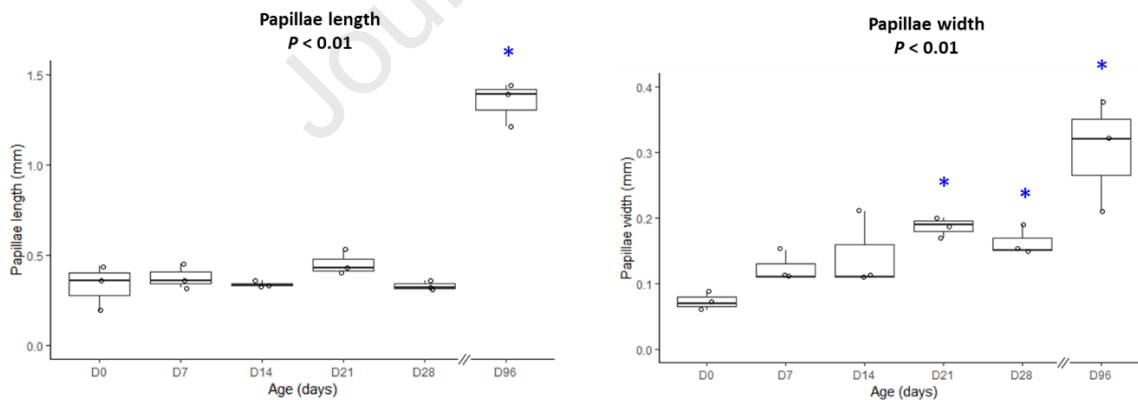
351

Journal Pre-proof

352 **A**

353

354

355 **B**

356

357

358 Fig. 1. Rumen papillae measurements at various ages. (A) Rumen tissues were taken from calves

359 at birth (D0), and 7 (D7), 14 (D14), 21 (D21), 28 (D28) and 96 d of age (D96). Sections were

360 stained with haematoxylin and eosin (HE) and imaged under a light microscope at 50 ×

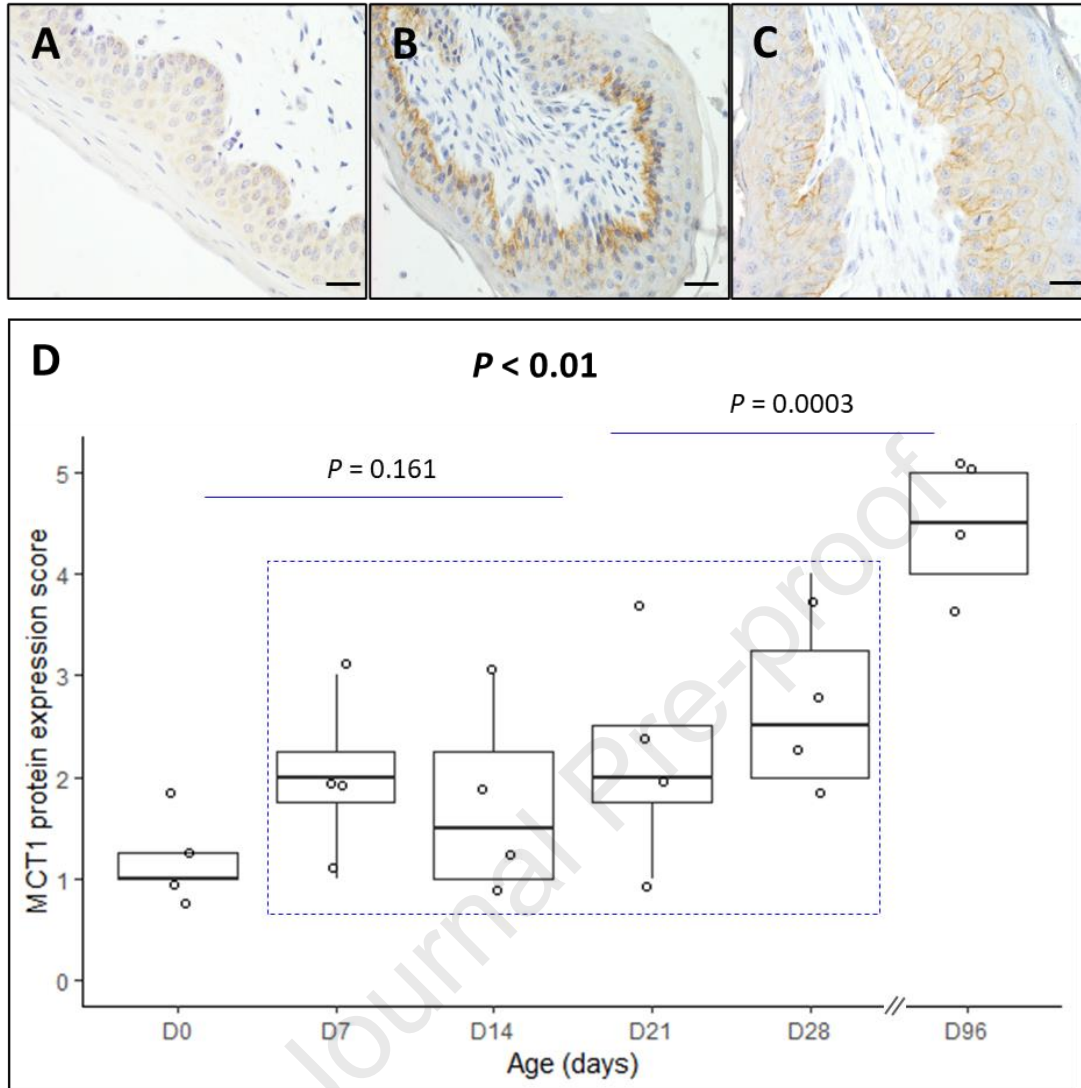
361 magnification (showing 1 set of tissues). Scale bar = 500 μm . (B) Ten papillae of each animal
362 were measured for length and width. Analysis of variance showed significant age dependent
363 difference for papilla length ($P < 0.01$, $n = 3$) and width ($P < 0.01$, $n = 3$). D96 calves had 4-fold
364 longer papillae than D0 (estimated means: 1.35 vs. 0.33 mm; $P < 0.01$), whereas the papilla
365 length of D7, D14, D21, and D28 were not significantly different from that of D0 ($P > 0.05$,
366 Tukey's HSD). The papillae width of D96 animals were 4-fold greater than D0 (estimated
367 means: 0.29 vs. 0.07 mm; $P < 0.01$, Tukey's HSD). The papillae of D28 ($P < 0.05$) and D21 ($P <$
368 0.01) were also wider than that of D0, but those of D14 and D7 were not significantly different
369 from D0 ($P > 0.05$, Tukey's HSD). * indicates statistical difference ($P < 0.05$) from D0.

370

371

372

373



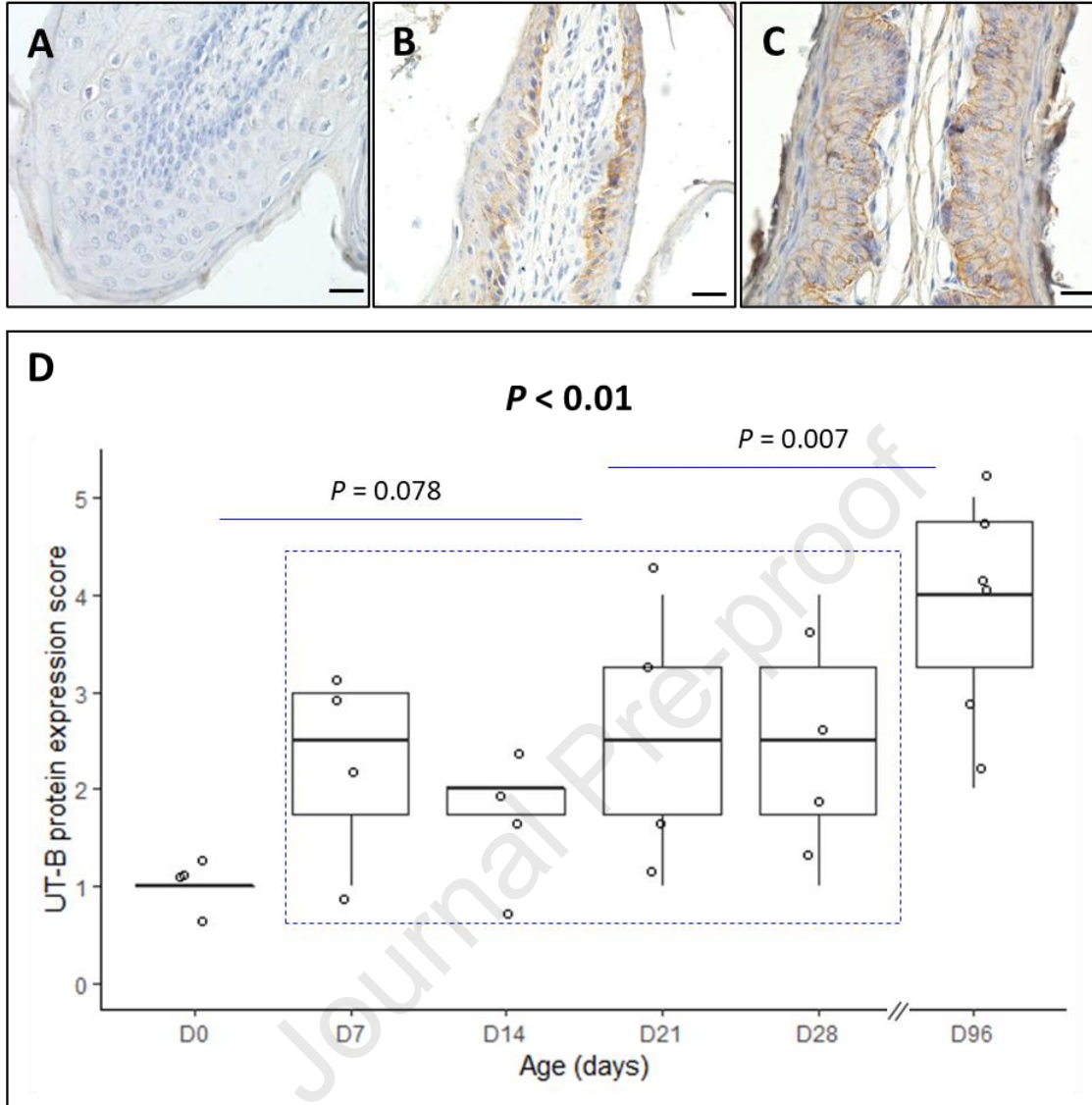
374

375

376 **Fig. 2.** Ruminal monocarboxylate transporter 1 (MCT1) protein localization and abundance
 377 across ages. Representative images showing the staining of MCT1 protein (brown) in the rumen
 378 epithelium of calves at birth (A), 28 (B) and 96 d of age (C). The cells were counterstained by
 379 haematoxylin to visualize nuclei (dark blue). Scale bar = 25 μ m. (D) Signal strength of 4 animals
 380 of each age group were blind scored by 3 examiners on a scale of 0 to 5, where 0 = none, 1 =
 381 very weak, 2 = weak, 3 = moderate, 4 = strong, 5 = very strong. D0, D7, D14, D21, D28 and

382 D96 represented at birth, 7, 14, 21, 28 and 96 d of age, respectively. Analysis of variance showed
383 statistical difference with ages ($P < 0.01$, $n = 4$).

Journal Pre-proof



384

385

386 Fig. 3. Ruminal urea transporter B (UT-B) protein localization and abundance across ages.

387 Representative images showing the staining of UT-B protein (brown) in the rumen epithelium of

388 calves at birth (A), 21 (B) and 96 d of age (C). Scale bar = 25 μ m. (D) Immunostaining strength

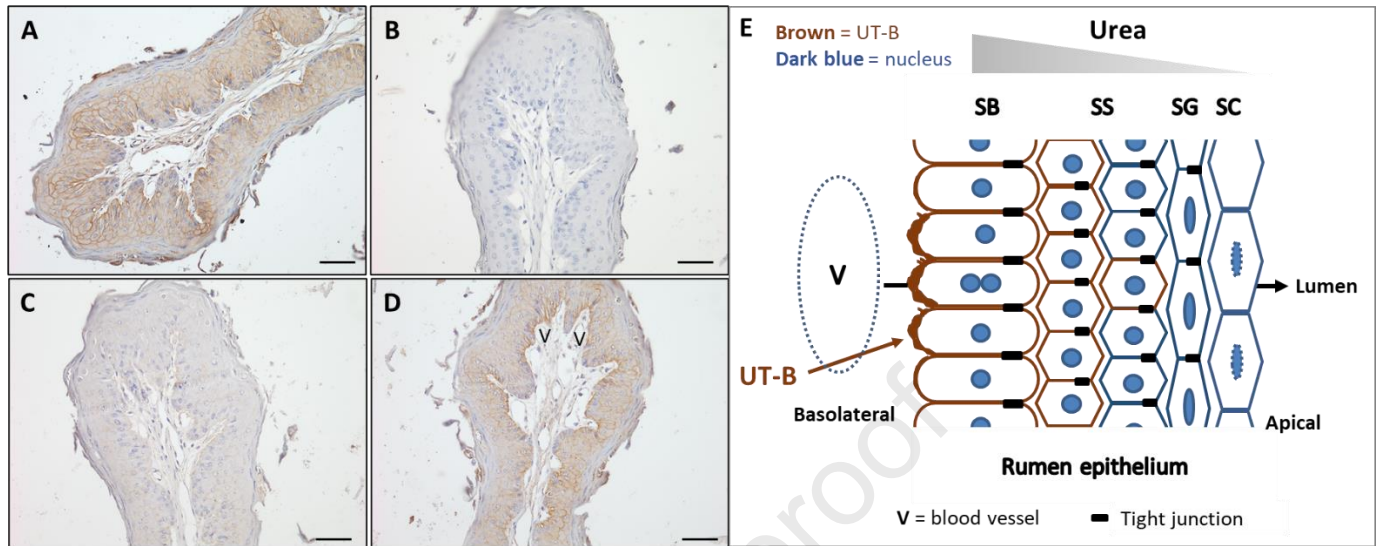
389 of 4 or 6 animals of each age group were blind scored by 3 examiners on a scale of 0 to 5, where

390 0 = none, 1 = very weak, 2 = weak, 3 = moderate, 4 = strong, 5 = very strong. D0, D7, D14, D21,

391 D28 and D96 represented at birth, 7, 14, 21, 28 and 96 d of age, respectively. Analysis of

392 variance showed significant difference of staining scores across ages ($P < 0.01$, $n = 4$ or 6).

393



394

395

396 Fig. 4. Primary antibody removal and peptide competition analysis showing the specificity of
 397 urea transporter B (UT-B) immunostaining in rumen tissue of calves at 96 d of age. (A) In the
 398 presence of the UT-B antibody and a corresponding secondary antibody, strong signals were
 399 detected at the stratum basale and the stratum spinosum. (B) In the absence of the UT-B
 400 antibody, but presence of the secondary antibody, no signals were generated. (C) Pre-absorption
 401 of the UT-B antibody with its specific immunizing peptide prevented most of the signals. (D) In
 402 contrast, pre-treatment with a similar amount of non-specific peptide had only a minimal effect
 403 on the signals, with the strongest intensity at the basolateral membrane facing blood vessels.
 404 Scale bar = 50 μ m. (E) Schematic diagram illustrating the general UT-B staining pattern across
 405 rumen epithelial layers. SB = stratum basale; SS = stratum spinosum; SG = stratum granulosum;
 406 SC = stratum corneum; V = blood vessel.

407

408

409